Fission Fragment Angular Distributions and Saddle Deformations*

R. CHAUDHRY,† R. VANDENBOSCH, AND J. R. HUIZENGA
Argonne National Laboratory, Argonne, Illinois

(Received November 20, 1961)

The fission fragment angular distributions have been measured with solid-state detectors for helium-ion-induced fission of bismuth, lead-206, thallium, and gold. The measurements were made at several helium-ion-projectile energies between 30 and 43 Mev. With 42.8-Mev helium ions the relative differential fission cross sections for gold and bismuth targets were measured at ten angles between 90° and 180° and the resulting angular distributions fitted by a least-squares method with Legendre polynomials. The $W(174.5°)/W(90°)$ ratios for 42.8-Mev helium-ion-induced fission of bismuth, lead, lead-206, thallium, and gold are 2.26 ± 0.07, 2.47 ± 0.08, 2.46 ± 0.08, 2.53 ± 0.08, and 2.62 ± 0.08, respectively. The relative fission cross sections at 174.5° and 90° were also measured at several lower helium-ion energies for all targets except natural lead. These data are utilized in the calculation of the energy dependence of K_0, the standard deviation of the distribution in the angular-momentum projection on the nuclear symmetry axis at the saddle point. The energy dependence of K_0 deduced from the experimental anisotropy measurements is similar to the predicted energy dependence from statistical theory if the nuclear temperature at the saddle point is proportional to the square root of the excitation energy. These results indicate that the effective moment of inertia is independent of excitation energy and they differ from heavy element (uranium region) results where it was found that at low excitation energies the experimental K_0 values were much reduced from statistical theory presumably due to pairing effects. With the assumption that the effective moment of inertia at the saddle point deformation (which is deduced for each target from the anisotropy measurement at the highest energy) is the rigid-body value, the stretching at the saddle point is calculated for various simple geometric configurations. For a saddle configuration of two equal tangent spheroids, the stretchings necessary to reproduce the observed effective moments of inertia are in good agreement with the liquid drop model calculations of Cohen and Swiatecki. Some comments are made on previous analyses of heavy-ion-induced fission of elements in the vicinity of gold.

I. INTRODUCTION

In recent years several investigations of fission fragment angular distributions have been reported. Most of these experiments were performed with heavy-element targets (uranium region), although a variety of projectiles were used to induce fission. Angular distributions of fission fragments from targets in the vicinity of lead bombarded with helium ions have been reported by Coffin and Halpern[1] and Nicholson.[2] The fission fragment angular distributions have been interpreted with the theory suggested by A. Bohr[3] and developed by Halpern and Strutinski[4] and Griffin.[5]

The aim of the present experiments is to derive information about the deformations at the saddle points for several fissioning nuclei in the vicinity of lead from an investigation of the angular distribution of fission fragments. Liquid drop model calculations[6,7] indicate a marked change in the deformation of the saddle point for elements with x between 0.65 and 0.74, where $x=(Z^2/A)/(Z^2/A)_{\text{crit}}$. Therefore, target elements of gold, thallium, lead, and bismuth were chosen in this investigation. The fission fragments were detected with solid-state junction counters. Since essentially all the fission for the above targets is first-chance fission, it is simpler to interpret their fission fragment anisotropies than those from heavy elements.

From the angular distributions measurements, the values of K_0^2 are evaluated for each compound nucleus as a function of excitation energy in excess of the fission barrier. The quantity K_0 is defined as the standard deviation of the distribution in angular momentum projection on the nuclear symmetry axis at the saddle point. The theory[4] postulates that the K distribution is that of the intrinsic states of the nucleus at the saddle-point excitation energy and is not altered at stages of the fission process beyond the saddle point. Some evidence[8] exists in support of this postulate. With the Fermi gas model and statistical arguments, the effective moments of inertia at the saddle deformations are deduced from the values of K_0^2. For independent-particle motion in an average nuclear field the moment of inertia has been shown to be that of a rigid body.[9–11] With the assumption that the compound nucleus at the saddle deformation for our highest excitation energy (above the fission barrier) can be represented by independent-particle motion, it is possible to evaluate the magnitude of the deformation at the saddle point from the angular distribution measurements. The saddle shapes are estimated by assuming simple geometric configurations and calculating the amount of deformation required to

* Based on work performed under the auspices of the U. S. Atomic Energy Commission.

† On leave from Atomic Energy Establishment, Trombay, India under sponsorship of the International Cooperation Administration.

[1] C. T. Coffin and I. Halpern, Phys. Rev. **112**, 536 (1958).

[2] W. J. Nicholson, Jr., Ph.D. thesis, University of Washington, 1960 (unpublished).

[3] A. Bohr, *Proceedings of the First United Nations International Conference on the Peaceful Uses of Atomic Energy* (United Nations, New York, 1956), Vol. 2, p. 151, Paper P/911.

[4] I. Halpern and V. M. Strutinski, *Proceedings of the Second United Nations International Conference on the Peaceful Uses of Atomic Energy* (United Nations, Geneva, 1958), Vol. 15, p. 408, Paper P/1513.

[5] J. J. Griffin, Phys. Rev. **116**, 107 (1959).

[6] S. Frankel and N. Metropolis, Phys. Rev. **72**, 914 (1947).

[7] S. Cohen and W. J. Swiatecki, Aarhus Universitet Report, 1961 (unpublished).

[8] R. Vandenbosch, H. Warhanek, and J. R. Huizenga, Phys. Rev. **124**, 846 (1961).

[9] H. A. Bethe, Rev. Modern Phys. **9**, 1 (1937); see discussion on page 84.

[10] C. Bloch, Phys. Rev. **93**, 1101 (1954).

[11] T. Ericson, Advances in Phys. **9**, 425 (1960).

TABLE I. Angular distributions of fission fragments from 42.8-Mev helium-ion-induced fission of Au^{197} and Bi^{209}. The coefficients a_i result from a least-squares fit to the experimental data given in Fig. 1.

Target	a_0	a_2	a_4	a_6	a_8	a_{10}
	$W(\theta)/W(90°)=a_0+a_2P_2(\cos\theta)+a_4P_4(\cos\theta)+a_6P_6(\cos\theta)$					
Au^{197}	1.3144±0.0265	0.8551±0.0518	0.3370±0.0684	0.0379±0.0721		
Bi^{209}	1.2546±0.0105	0.6925±0.0204	0.2389±0.0268	0.0771±0.0284		
	$W(\theta)/W(90°)=a_0+a_2P_2(\cos\theta)+a_4P_4(\cos\theta)+a_6P_6(\cos\theta)+a_8P_8(\cos\theta)+a_{10}P_{10}(\cos\theta)$					
Au^{197}	1.3146±0.0325	0.8539±0.0636	0.3370±0.0849	0.0348±0.1013	−0.0086±0.1126	0.0195±0.1149
Bi^{209}	1.2530±0.0077	0.6930±0.0150	0.2284±0.0200	0.0524±0.0238	0.0695±0.0263	−0.0164±0.0270

reproduce the effective moment of inertia. These results are compared with the liquid drop model calculations of Cohen and Swiatecki.[7]

The dependence of the effective moment of inertia on excitation energy is also of interest. In the case of heavy-element targets (uranium region) the effective moment of inertia at the saddle point is reduced[1,4,8,12] at low excitation energies presumably due to pairing correlations. Liquid drop model calculations[7] predict that the saddle configurations of the elements under study are considerably different from the uranium nuclei. An investigation has therefore been made of the energy dependence of the fission fragment angular distributions in order to determine the effect of saddle deformation on the energy dependence of the effective moment of inertia at the saddle point.

II. EXPERIMENTAL PROCEDURE

The experimental arrangement, targets, fission fragment detectors, and counting procedures are identical with those reported in our previous paper.[13]

III. EXPERIMENTAL RESULTS

The fission fragment angular distributions (or relative differential fission cross section as a function of angle) were measured for Au^{197} and Bi^{209} targets bombarded with 42.8-Mev helium ions in the laboratory system. One detector was fixed at 186° to the beam direction and the second detector was rotated from 85° to 174° to the beam in several steps. The first detector served as a monitor. The normal to the target bisected the angle between the two detectors in all runs. The laboratory counting rates and angles were converted to the corresponding center-of-mass values with the assumption of full momentum transfer[14] of the helium ions to the compound nucleus. The fission fragments were assumed to have energies[15] equal to the average energy of 70 Mev for the compound nucleus Tl^{201} and 74 Mev for the compound nucleus At^{213}. The measured angular distributions for both the above targets are plotted in the center-of-mass system in Fig. 1.

As discussed previously[16] for other targets, the angular distributions cannot be reproduced with an equation of the form, $W(\theta)=a+b\cos^2\theta$. Least-squares fits to the experimental data were determined with Legendre polynomials with terms up to $P_6(\cos\theta)$ and with terms up to $P_{10}(\cos\theta)$. The coefficients resulting from each least-squares fit for both the Au^{197} and Bi^{209}

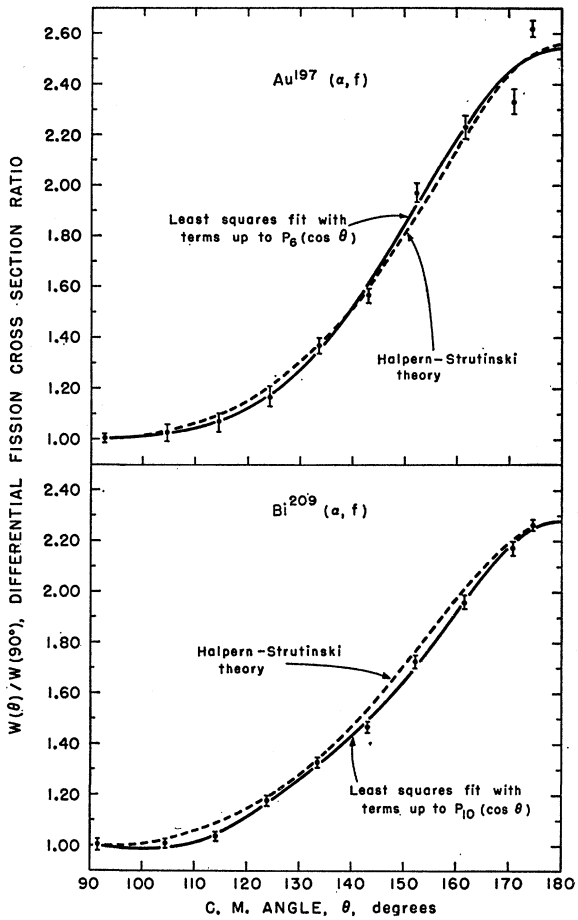

FIG. 1. Ratio of the differential fission cross section $W(\theta)/W(90°)$, as a function of the center-of-mass angle in degrees. The points are the experimental data. The solid lines are the least-squares fit to the experimental data. The dashed lines are calculated from the Halpern-Strutinski theory (normalized to least-squares curve at 174.5°).

[12] J. J. Griffin, *Proceedings of the International Conference on Nuclear Structure, Kingston, Canada, 1960* (University of Toronto Press, Toronto, 1960), p. 843.

[13] J. R. Huizenga, R. Chaudhry, and R. Vandenbosch, preceding paper [Phys. Rev. **126**, 220 (1962)].

[14] W. J. Nicholson and I. Halpern, Phys. Rev. **116**, 175 (1959).

[15] R. Vandenbosch and J. R. Huizenga (to be published).

[16] J. R. Huizenga, R. Vandenbosch, and H. Warhanek, Phys. Rev. **124**, 1964 (1961).

TABLE II. Ratio of differential fission cross sections at 174.5° and 90° $[W(174.5°)/W(90°)]$ in the center-of-mass system for several targets bombarded with 42.8-Mev (laboratory energy) helium ions.

Cycle \ Target	Au^{197}	$Tl^{203,205}$ (natural)	Pb^{206} (enriched to 88%)	Pb (natural)	Bi^{209}
1	2.66±0.06	2.57±0.06	2.50±0.06	2.49±0.05	2.25±0.04
2	2.69±0.06	2.62±0.05	2.45±0.06	2.49±0.05	2.33±0.04
3	2.51±0.05	2.40±0.05	2.44±0.05	2.42±0.05	2.31±0.04
4					2.17±0.04
Average	2.62±0.03[a] ±0.08[b]	2.53±0.03 ±0.08	2.46±0.03 ±0.08	2.47±0.03 ±0.08	2.26±0.02 ±0.07

[a] Statistical error.
[b] Includes systematic errors in addition to random error.

targets are summarized in Table I. As can be seen from the data in Table I, the coefficients of some of the higher terms are not statistically significant. In Fig. 1, the least-squares fit for Au^{197} with terms up to $P_6(\cos\theta)$ and for Bi^{209} with terms up to $P_{10}(\cos\theta)$ are plotted.

The ratios of the differential fission cross sections at the center-of-mass angles of 174.5° and 90° were measured for 42.8-Mev helium-ion bombardments of Au^{197}, natural Tl, Pb^{206} (enriched to 88%), natural lead, and Bi^{209}. The cross sections for the two angles were measured simultaneously, thereby eliminating any error in the integrated beam current. The fission cross section ratio of a particular target was determined with a statistical error of about 2% and then the target was changed. The five targets were rotated through three complete cycles and the individual results are tabulated in Table II. The average values of the ratios have statistical errors of about 1%. The individual results fluctuate outside the statistical error due to systematic errors, the largest of which is the shift of the beam current position on the target. The last line in Table II gives an estimate of total error in the cross section ratio of about 3%. These larger errors are included in all estimates of the saddle-shape stretching from the anisotropy measurements.

The ratios of the differential fission cross sections at the center-of-mass angles of 174.5° and 90° were measured for reduced energy helium-ion bombardments of Au^{197}, natural Tl, Pb^{206} (enriched to 88%), and Bi^{209}. The results are summarized as a function of helium-ion energy in the laboratory system (and as a function of excitation energy in the center-of-mass system) in Table III. The errors listed in Table III include only the statistical counting errors at both angles. In order to obtain the relatively small statistical errors listed in Table III for the lower energies where the fission cross section is very small, several hours of bombardment time were required for each energy. The binding energies of helium ions to targets employed in this study which were used in computing the excitation energies were taken from the compilation of Everling *et al.*[17]

IV. DISCUSSION

A. Calculation of K_0^2 and Effective Moment of Inertia at the Saddle Deformation

Halpern and Strutinski[4] have developed the theory of angular distributions for fission fragments from particle-induced fission at medium energies. They have given an expression for the differential cross section at angle

TABLE III. Ratio of differential fission cross sections at 174.5° and 90° in the center-of-mass system for several targets as a function of helium-ion-bombarding energy in the laboratory system in Mev (and also as a function of excitation energy in the center-of-mass system in Mev).

Au^{197}			$Tl^{203,205}$ (natural)			Pb^{206} (enriched to 88%)			Bi^{209}		
$E_{(lab)}$	E	$W(174.5°)/W(90°)$	$E_{(lab)}$	E	$W(174.5°)/W(90°)$	$E_{(lab)}$	E	$W(174.5°)/W(90°)$	$E_{(lab)}$	E	$W(174.5°)/W(90°)$
42.8	40.5	2.62±0.03	42.8	38.8	2.53±0.03	42.8	36.6	2.46±0.03	42.8	32.6	2.26±0.02
42.7	40.4	2.55±0.05	39.6	35.6	2.68±0.18	42.3	36.1	2.55±0.11	42.6	32.4	2.29±0.04
41.2	38.5	2.43±0.13	35.7	31.8	2.57±0.30	39.8	33.6	2.45±0.11	40.8	30.7	2.28±0.04
38.8	36.5	2.41±0.13				38.1	32.0	2.57±0.14	39.5	29.4	2.23±0.04
36.8	34.6	2.55±0.21				36.0	29.9	2.51±0.15	38.7	28.6	2.29±0.04
35.1	32.9	2.56±0.22				33.9	27.8	1.73±0.23	38.0	27.9	2.25±0.03
33.3	31.1	2.23±0.23							37.4	27.3	2.17±0.05
									36.6	26.5	2.21±0.04
									36.0	25.9	2.17±0.06
									35.1	25.1	2.30±0.05
									34.2	24.2	2.27±0.10
									33.1	23.1	2.19±0.05
									32.4	22.4	2.09±0.17
									31.3	21.3	2.06±0.11
									30.7	20.7	1.82±0.22

[17] F. Everling, L. A. König, J. H. E. Mattauch, and A. H. Wapstra, Nuclear Phys. 18, 529 (1960).

θ as

$$W(\theta)=(2/\pi)^{\frac{1}{2}}\frac{N}{2\pi}\int_0^{I_m^2}\frac{I}{2K_0}\times\exp\left(\frac{-I^2\sin^2\theta}{4K_0^2}\right)J_0\left(\frac{iI^2\sin^2\theta}{4K_0^2}\right)dI^2. \quad (1)$$

Making the substitutions, $p=(I_m/2K_0)^2$ and $x=(I\sin\theta/2K_0)^2$, the above expression can be written in the form,

$$\frac{W(\theta)}{W(90°)}=\sin^{-3}\theta\left[\int_0^{p\sin^2\theta}x^{\frac{1}{2}}\exp(-x)J_0(ix)dx\Big/\int_0^{p}x^{\frac{1}{2}}\exp(-x)J_0(ix)dx\right]. \quad (2)$$

In the above expression θ is the center-of-mass angle of the fission fragment with respect to the incident beam, I_m is the maximum angular momentum brought in by the incident particles, J_0 is the zero-order Bessel function, and K_0 is the standard deviation of the distribution in the angular-momentum projection on the nuclear symmetry axis at the saddle point. The expression for the differential fission cross section relative to that at 90° given by Eq. (2) has the simplifying assumptions that the distribution in K is Gaussian and the distribution $F(I)$ is proportional to I and the target spin is negligible.

The actual distribution of I may be rounded instead of having a sharp cutoff at I_m, but by choosing $I_m^2=2\langle I^2\rangle_{\text{av}}$, Eq. (2) may be made insensitive[8] to the actual distribution $F(I)$. The values of $W(\theta)/W(90°)$ were evaluated from Eq. (2) at various angles for various values of p on a computer. The spins of the four targets Au^{197}, $Tl^{203,205}$, Pb^{206}, and Bi^{209} are $\frac{3}{2}$, $\frac{1}{2}$, 0, and $\frac{9}{2}$, respectively. Calculations indicate that even for Bi^{209} the effect of the target spin on the anisotropy is very small and hence the assumption implicit in Eq. (2), that the target spin is negligible, is thought to be valid. In the cross section measurements reported previously,[13] it has been shown that second-chance fission is less than 3% at all excitation energies for the compound nuclei investigated. Therefore, the effect of second-chance fission has been neglected in the calculations of anisotropies.

Measurements of complete angular distributions were performed for two targets at our maximum projectile energy of 42.8 Mev. Choosing a p value which reproduces the least-squares fit at 90° and 174°, we have computed from Eq. (2) the expected angular distribution for intermediate angles. The agreement with experiment is illustrated in Fig. 1 and considered quite satisfactory.

Most of the differential fission cross section measurements were made at 90° and 174.5° in the center-of-mass system. Experiments were performed at various bombarding energies for all targets studied, with particular emphasis on the targets Au^{197} and Bi^{209}. The experimental values of $W(174.5°)/W(90°)$ and values of $\langle I^2\rangle_{\text{av}}$ from optical model transmission coefficient calculations enabled us to deduce values of K_0^2 as a function of the projectile energies. These K_0^2 values are plotted against the excitation energy in excess of the fission threshold in Fig. 2 for the compound nuclei Tl^{201} and At^{213}. The fission thresholds[13], E_f', for Tl^{201}, $Bi^{207,209}$, Po^{210}, and At^{213} are 19.9±2.0, 20.6±2.0, 19.7±2.0, and 15.8±2.0 Mev, respectively. The quantity E_f' is the energy which must be supplied to a ground-state nucleus to reach the point at which the saddle-level density is initiated.

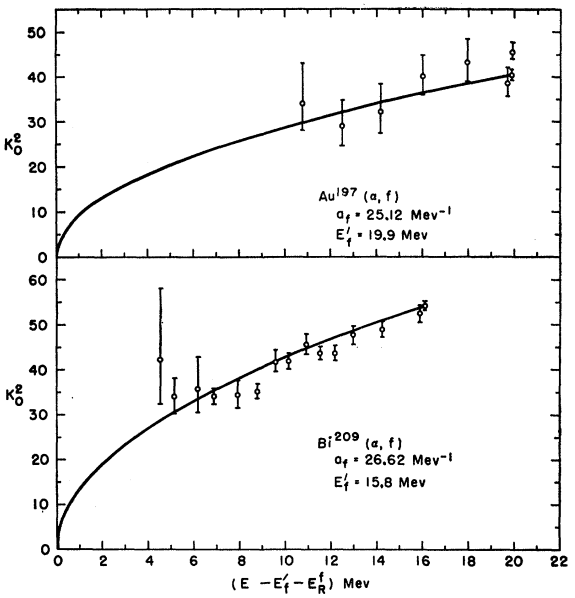

FIG. 2. Energy dependence of the fission fragment anisotropy for helium-ion-induced fission of gold and bismuth. The values (open circles) of K_0^2 deduced from the anisotropies are plotted as a function of excitation energy above the fission barrier. The solid curve gives the theoretical energy dependence for a Fermi gas model (normalized at highest energy point).

From rather general statistical theory considerations[4,5] and the use of a Fermi gas model one can show that K_0^2 is given by

$$K_0^2=\frac{T}{\hbar^2}\frac{\mathcal{I}_\perp\mathcal{I}_{||}}{\mathcal{I}_\perp-\mathcal{I}_{||}}, \quad (3)$$

where T is the nuclear temperature given by $[(E-E_f'-F_R{}^f)/a_f]^{\frac{1}{2}}$, $E_R{}^f$ is the rotational energy at the saddle point,[13] and $\mathcal{I}_\perp$ and $\mathcal{I}_{||}$ are the moments of inertia of the nucleus at the saddlepoint, perpendicular and parallel to the nuclear symmetry axis, respectively. The effective moment of inertia $\mathcal{I}_{\text{eff}}$ is defined as

$$\mathcal{I}_{\text{eff}}=\mathcal{I}_\perp\mathcal{I}_{||}/(\mathcal{I}_\perp-\mathcal{I}_{||}). \quad (4)$$

The solid lines in Fig. 2 represent the excitation energy dependence of K_0^2 given by Eq. (3) after normalizing to the highest excitation energies in each case. It can be seen that the experimental points fall within

TABLE IV. Deformation of the fissioning nucleus at the saddle point derived from the experimentally determined values of K_0^2 for three simple geometric configurations. In all of these calculations $r_0=1.216\times10^{-13}$ cm and $a_f=A/8$.

Compound nucleus	x[a]	$E-E_f'-E_R'$ (Mev)	$\mathcal{I}_{\text{eff}}/\mathcal{I}_{\text{sph}}$	One spheroid[c,f] C'/A'	One spheroid[c,f] $R_{\max}/R_0$	Two spheroids[d,f] C/A	Two spheroids[d,f] $R_{\max}/R_0$	Two cones with hemispherical caps[e,f] r/h	Two cones with hemispherical caps[e,f] $R_{\max}/R_0$
Tl^{201}	0.651	19.9	0.468±0.031	3.84±0.27	2.45±0.11	1.82±0.14	2.36±0.12	0.317±0.039	3.03±0.22
Bi^{209} [b]	0.657	17.5	0.504±0.033	3.55±0.23	2.33±0.10	1.67±0.12	2.24±0.10	0.363±0.044	2.81±0.18
Po^{210}	0.670	16.2	0.552±0.036	3.25±0.20	2.19±0.09	1.52±0.11	2.09±0.10	0.428±0.050	2.58±0.16
At^{213}	0.677	16.1	0.648±0.042	2.81±0.015	1.99±0.07	1.30±0.08	1.89±0.08	0.573±0.070	2.23±0.13
Pu^{237}	0.744	31.3	1.21 ±0.15	1.85±0.12	1.51±0.06	0.81±0.06	1.38±0.06	1.59 ±0.28	1.49±0.08

[a] $x=(Z^2/A)/(Z^2/A)_{\text{crit}}$, where $(Z^2/A)_{\text{crit}}=50.13$.
[b] Target material was natural thallium.
[c] C' and A' are the lengths of the major and minor axes of a prolate spheroid.
[d] C and A are the lengths of the major and minor axes of one of the two tangent prolate spheroids.
[e] Two identical cones joined base to base along their axes and each capped with an identical hemisphere; r is the radius of the hemisphere and h the height of each cone.
[f] R_0 is the radius of a single sphere containing the incompressible matter.

the statistical errors on the predicted curves indicating that $\mathcal{I}_{\text{eff}}$ is independent of excitation energy. This is in contrast to the case for the heavier elements where for excitation energies above threshold of less than 7–11 Mev the observed values of K_0^2 are depressed considerably from the simple dependence of Eq. (3). In the case of the heavier elements Griffin[12] has had fair success in accounting for the depression of K_0^2 by taking into account pairing effects which reduce the moments of inertia from their rigid-body values. As will be discussed later, liquid drop model calculations suggest that the less fissionable elements may have saddle-point configurations which resemble two spheroids joined by a thin neck rather than the one spheroid (or cylindrical) thick-necked configuration thought to occur for the heavier elements. If the saddle-point configuration resembles two spheroids in contact, most of the contribution to $\mathcal{I}_\perp$ must come from a term mr^2 corresponding to the translation of the individual spheroid axes of rotation to an axis at the point of contact of the two spheroids. Thus the pairing can only act effectively on $\mathcal{I}_{\text{II}}$ and the dependence of temperature on excitation energy. One might expect then that the K_0^2 values for lighter elements will be depressed less than the K_0^2 values for heavier elements because of the difference in the saddle-point configurations.

B. Saddle Deformations

Simple models of nuclear structure have been used to show that at high excitation energies nuclear moments of inertia are equal to those for rigid rotation.[9–11] Using this result, it is possible to deduce information about the shape of the saddle-point configuration from the K_0^2 values obtained from the anisotropy measurements. The procedure is to assume a value for a_f and hence for the temperature, and then, for various families of simple geometrical shapes, deduce the parameters which will reproduce the effective moment of inertia. In these calculations the $W(174.5°)/W(90°)$ ratio summarized in Table II were used to calculate K_0^2. It is convenient to give the effective moments of inertia at the saddle point, which are calculated from the experimentally determined values of K_0^2 and listed in column 4 of Table IV, in units of the moment of inertia of a sphere of the same volume. The nuclear radius[18] has been taken as $R=r_0A^{\frac{1}{3}}$ with $r_0=1.216$ fermi, and a_f has been assumed equal to $A/8$. The excitation energies at which K_0^2 was determined are summarized in column 3, and the stretching parameters which are derived are summarized in columns 5 to 10 of Table IV. The fifth column contains the ratio of the major to minor axes (C'/A') for a single axially symmetric prolate spheroid which reproduces the effective moment of inertia. The sixth column lists for a one-spheroid saddle point the ratio of the maximum radius (one-half of the entire major axis) to the radius of a sphere of the same volume. Parameters are given in the seventh and eighth columns for a saddle-point configuration of two equal tangent prolate spheroids joined along their major axes. The values of C/A are the ratios of the major to minor axes for the individual spheroids. The values of $R_{\max}/R_0$ again refers to the ratio of the maximum radius of the system (entire major axis of one of the spheroids) to the radius of a sphere of the same volume. The parameters given in the ninth and the tenth columns are for a saddle-point configuration of two identical cones with hemispherical caps which are joined at their vortexes. The parameters calculated from anisotropy measurements[8] for the heavy nucleus Pu^{237} are included in Table IV for comparison.

The stretching parameter $R_{\max}/R_0$ is plotted against $\mathcal{I}_{\text{eff}}/\mathcal{I}_{\text{sph}}$ in Fig. 3 for three different saddle-point configurations. It is interesting to note that for a particular value of $\mathcal{I}_{\text{eff}}/\mathcal{I}_{\text{sph}}$, the one- and two-spheroid saddle point configurations give about the same stretching for small values of $\mathcal{I}_{\text{eff}}/\mathcal{I}_{\text{sph}}$, although the two-spheroid values are slightly smaller. The stretchings with the saddle configuration of two cones with hemispherical caps are considerably larger for small values of $\mathcal{I}_{\text{eff}}/\mathcal{I}_{\text{sph}}$. However, when $\mathcal{I}_{\text{eff}}/\mathcal{I}_{\text{sph}}$ approaches unity, the $R_{\max}/R_0$ value of the two-cone saddle shape approaches the value of the one-spheroid saddle shape and the stretchings

[18] A. E. S. Green, Phys. Rev. **95**, 1006 (1954); Revs. Modern Phys. **30**, 569 (1958).

for the two models become equal at $\mathcal{I}_{\text{eff}}/\mathcal{I}_{\text{sph}}$ of about 1.1.

The errors in the quantity $\mathcal{I}_{\text{eff}}/\mathcal{I}_{\text{sph}}$ are derived from the uncertainty of ± 0.08 in the $W(174.5°)/(W90°)$ ratios given in Table II. The errors listed in columns 5 to 10 are in turn calculated from the errors in the $\mathcal{I}_{\text{eff}}/\mathcal{I}_{\text{sph}}$ ratios and illustrate the error in the stretching associated with a particular error in the effective moment of inertia.

Before comparing the saddle deformations which are summarized in Table IV with liquid drop model calculations, the sensitivity of the saddle deformations to the nuclear radius parameter r_0 and to the level density parameter a_f at the saddle deformation will be discussed. Since $\mathcal{I}_{\text{eff}}/\mathcal{I}_{\text{sph}}$ is inversely proportional to the square of the nuclear radius parameter, an increase in r_0 causes a decrease in the value of $\mathcal{I}_{\text{eff}}/\mathcal{I}_{\text{sph}}$ and an increase in the saddle-point stretching. For example, if r_0 is increased by 10%, the value of $R_{\max}/R_0$ (for the saddle point of two equal, tangent prolate spheroids) is increased by 17% for Tl^{201}. Since the effective moment of inertia at the saddle point is proportional to the square root of a_f, a decrease in a_f reduces the value of $\mathcal{I}_{\text{eff}}/\mathcal{I}_{\text{sph}}$, and hence increases the saddle-point stretching. For example, if a_f is reduced by 20%, the value of $R_{\max}/R_0$ (for the two-equal-tangent prolate spheroid saddle point) is increased for Tl^{201} by 9.6%.

A further comment should be made about the relationship between $\mathcal{I}_{\text{eff}}/\mathcal{I}_{\text{sph}}$ and the spin distribution of the compound nucleus. Each value of K_0^2 which is determined for each nucleus from the fission fragment anisotropy is directly proportional to I_m^2, which in the present calculation is chosen equal to $2\langle I^2\rangle_{\text{av}}$. The value of $\langle I^2\rangle_{\text{av}}$ was determined from optical model transmission coefficients.[19] Therefore, a 10% increase in $\langle I^2\rangle_{\text{av}}$ will increase K_0^2 by 10% and hence also increase $\mathcal{I}_{\text{eff}}/\mathcal{I}_{\text{sph}}$ by 10%. This decreases $R_{\max}/R_0$ (for the saddle point of two equal, tangent prolate spheroids) by 6.7% for Tl^{201}.

An upper limit on the stretching at the saddle point, and hence an upper limit on the value of r_0 or a lower limit on a_f, may be estimated from kinetic energy measurements. It is assumed that the kinetic energy arises from the Coulomb interaction energy at the scission configuration and that no kinetic energy is developed in passage from the saddle point to the scission configuration. If the scission configuration is represented by two equal, tangent prolate spheroids the ratio of the major to minor axes, C/A, derived from the kinetic energy measurements[15] is approximately constant and equal to 2.16 ± 0.10 ($R_{\max}/R_0=2.65$) for all nuclei for $r_0=1.216\times 10^{-13}$ cm. (The scission shape of Tl^{201}, Bi^{209}, Po^{210}, and At^{213} should be fairly well represented by two equal spheroids since all of these nuclei exhibit symmetric mass distributions.) If one requires that the saddle stretching be less than or equal to the scission stretching, it is possible to put limits on the parameters r_0 and a_f required to deduce $\mathcal{I}_{\text{eff}}/\mathcal{I}_{\text{sph}}$ from the measured values of K_0^2. Such a criterion requires that if $r_0=1.216\times 10^{-13}$ cm, then a_f must be greater than 19 Mev^{-1}, and conversely if $a_f=A/8$, r_0 must be less than 1.31×10^{-13} cm.

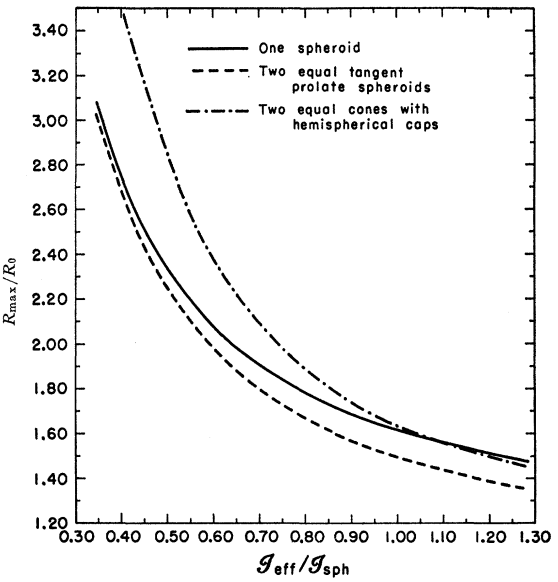

FIG. 3. Stretchings at the saddle deformation as a function of the effective moment of inertia for three simple geometric configurations. $R_{\max}$ is the maximum radius of the saddle shape and R_0 and $\mathcal{I}_{\text{sph}}$ are the radius and rigid-body moment of inertia of a sphere of the same volume.

C. Comparisons with the Liquid Drop Model

The only model from which a serious attempt has been made to calculate fission thresholds and saddle-point configurations is the charged liquid drop model. In this model the nuclear forces, idealized as a surface tension, tend to stabilize the nucleus in a spherical shape, while the Coulombic forces tend to deform the nucleus so as to reduce the Coulombic repulsion of the protons. Certainly this idealization of the very complicated nuclear interactions cannot be expected to account for the details of the fission process and may not even reproduce the gross aspects of the fission process. At the present stage of development of the liquid drop model, one cannot really say whether it is successful or not. Mathematical difficulties have made it impossible to make exact calculations of the potential energy surface, and only a first attempt has been made to incorporate the dynamics of the problem.

Recent calculations by Cohen and Swiatecki[7] of the potential energy surface in the region of the saddle-point configuration have led to some important changes in the conventional picture of fission. It appears that for values of the fissionability parameter $x=(Z^2/A)/$

[19] J. R. Huizenga and G. J. Igo, Nuclear Phys. **29**, 462 (1962); Argonne National Laboratory Report ANL-6373, 1961 (unpublished).

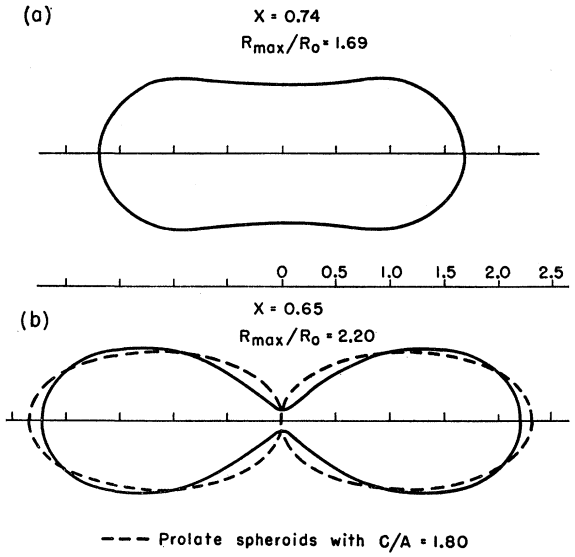

FIG. 4. Saddle shapes calculated by Frankel and Metropolis for $x=0.74$ and 0.65, where $x=(Z^2/A)/(Z^2/A)_{\text{crit}}$. (a) The one-spheriod thick-necked saddle configuration is thought to be an adequate representation of heavy element fission. (b) Saddle shapes for nuclei in the vicinity of $x=0.65$ were first approximated as two spheroids by Swiatecki.

$(Z^2/A)_{\text{crit}}$ greater than a certain value, the stages in the fission process might be represented schematically by the following sequence:

$$\text{equilibrium shape} \xrightarrow{\text{saddle}} \text{intermediate stage} \xrightarrow{\text{saddle}} \text{two fragments}$$

rather than the simpler sequence,

$$\text{equilibrium shape} \xrightarrow{\text{saddle}} \text{two fragments.}$$

The x value for which the two saddles may appear is at present not known exactly but may be in the region where x is greater than 0.68 to 0.70. For a $(Z^2/A)_{\text{crit}}$ value of 50.1, the x values for the nuclei under study are 0.65 to 0.68. This is very close to the region where one might expect rather large changes in the saddle-point configurations, as is illustrated in Fig. 4 by the calculations of Frankel and Metropolis[6] for $x=0.65$ and $x=0.74$. The more recent saddle-shape calculations of Swiatecki[20] for $x=0.74$ are not significantly different from the Frankel-Metropolis result. In addition, Swiatecki[7] has pointed out that for $x=0.65$ the saddle shape of two equal, tangent prolate spheroids with $C/A=1.80$ is very similar to the saddle shape calculated by Frankel and Metropolis.[6] The striking resemblance between the two configurations is illustrated in Fig. 4(b).

The saddle point of Tl^{201} is probably quite adequately represented by the two-spheroid shape. While such a description may not represent the saddle shape of At^{213} nearly so well, it probably is a superior representation to the thick-necked one-spheroid saddle representation. The values of $R_{\max}/R_0$ for the two-spheroid saddle shapes of Tl^{201}, Bi^{209}, Po^{210}, and At^{213} which are listed in column 8 of Table IV are plotted in Fig. 5 as a function of x. The dashed curve represents the best estimate of Cohen and Swiatecki[7] for the behavior of $R_{\max}/R_0$ as a function of x. In Fig. 5 the circles are from calculations of Frankel and Metropolis,[6] whereas the squares are from calculations of Cohen and Swiatecki.[7] The important point of this comparison is not the degree of quantitative agreement between the experimental and liquid drop model calculations of $R_{\max}/R_0$, but rather the observation that the experimental values of $R_{\max}/R_0$ are changing rapidly with x in the region predicted by the liquid drop model calculations. The value of $R_{\max}/R_0$ for Pu^{237} calculated on the basis of a one-spheroid saddle shape is also included in Fig. 5. For the heavy element Pu^{237}, the value of $R_{\max}/R_0$ calculated for a two-spheroid saddle is considerably below the dashed curve.

D. Further Implications of the Present Results

Several experiments[21,22] have been performed in which angular distributions for heavy-ion-induced fission of gold and bismuth have been obtained. From these experiments attempts have been made to conclude [21,22] whether fission occurs early or late in the evaporation chain, i.e., whether fission precedes neutron emission or whether neutron emission precedes fission. The argument goes as follows: From the measured anisotropy

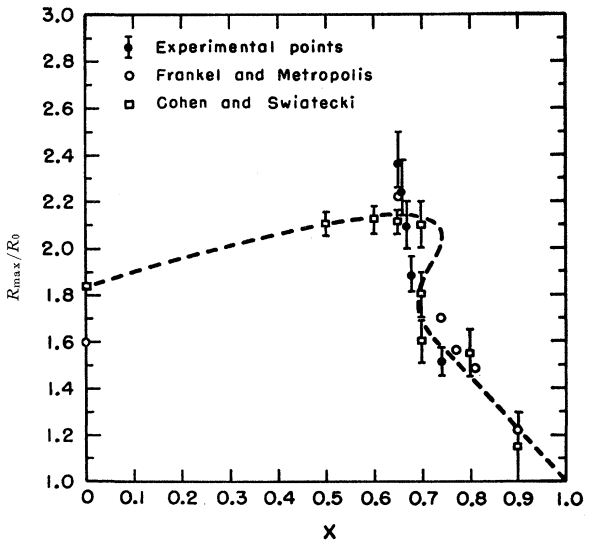

FIG. 5. Comparison of the determined values of $R_{\max}/R_0$ (solid circles) for Tl^{201}, Bi^{209}, Po^{210}, At^{213}, and Pu^{237} with liquid drop model calculations of the same quantity by Frankel and Metropolis (open circles) and Cohen and Swiatecki (open squares). The dashed curve is the best estimate of Swiatecki for the quantity $R_{\max}/R_0$ as a function of x, where $x=(Z^2/A)/(Z^2/A)_{\text{crit}}$.

[20] W. J. Swiatecki, Phys. Rev. **104**, 993 (1956); *Proceedings of the Second United Nations International Conference on the Peaceful Uses of Atomic Energy* (United Nations, Geneva, 1958), Vol. 15, p. 248, Paper P/651.

[21] G. E. Gordon, A. E. Larsh, T. Sikkeland, and G. T. Seaborg, Phys. Rev. **120**, 1341 (1960).

[22] H. C. Britt and A. R. Quinton, Phys. Rev. **120**, 1768 (1960).

and the known (in principle) I distribution one can obtain K_0^2 directly. One then looks at the K_0^2 versus $E-E_f$ curves for the heavy elements and deduces the average excitation energy at which fission has occurred. It is realized that fission actually does not occur at a single excitation energy but competes with neutron emission at almost every step of the evaporation chain, and thus one only gets an average excitation energy at which fission occurs. The point we wish to make here is that since the saddle-point configurations are considerably different for the lighter elements than for the heavier elements, it is improper to use the K_0^2 vs $E-E_f$ relationship obtained from heavy elements. For example, the compound nucleus formed from C^{12} bombardments of Au^{197} is At^{209}, a lighter isotope of the same element as the compound nucleus At^{213} which is formed in helium-ion-induced fission of Bi^{209}. The Z^2/A values of the lighter astatine isotopes are slightly higher than At^{213} and one would expect a K_0^2 value at a given excitation energy intermediate to At^{213} and the heavy elements. The line in Fig. 6 represents an interpolation of K_0^2 at $E-E_f=16$ Mev for various values of $x=(Z^2/A)/(Z^2/A)_{\text{crit}}$ between the bismuth and uranium regions. A sharp rise in K_0^2 at $x\approx 0.68$ is suggested both by the experimental anisotropies of the four targets studied and by the liquid drop model calculations. If one takes K_0^2 from this interpolation for the fissioning astatine isotope and assumes an excitation energy dependence for K_0^2 given by Eq. (3), one concludes that fission occurs at a higher average excitation energy than the surprisingly low values ($F-E_f=9$–13.5 Mev) previously suggested[21] and also one obtains a more reasonable variation with C^{12} bombarding energy than was found previously. It should be remarked that this type of analysis is independent of uncertainties in the level density parameters a_n and a_f, and the radius parameter r_0. The analysis is however complicated by the large angular momenta brought in by heavy ions, and the fact that fission can occur at various stages of the de-excitation process.

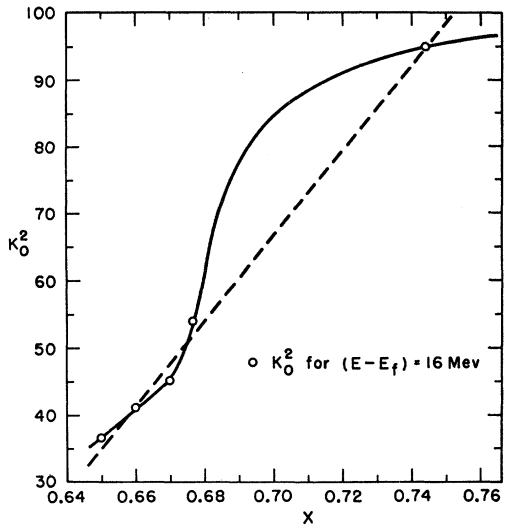

FIG. 6. Experimentally determined values (open circles) of K_0^2 for Tl^{201}, Bi^{209}, Po^{210}, At^{213}, and Pu^{237} at an excitation energy $(E-E_f)$ of 16 Mev plotted as a function of x, where $x=(Z^2/A)/(Z^2/A)_{\text{crit}}$. The dashed curve is a straight line drawn between the points, whereas the solid line is a best guess of the relationship between K_0^2 and x.

These difficulties make analysis of angular distributions for heavy-ion-induced fission almost meaningless.

ACKNOWLEDGMENTS

The authors wish to thank J. Scherer for his assistance with the computer calculations, W. Swiatecki for helpful conversations and members of the cyclotron group for operation of the cyclotron. One of us (R. Chaudhry) wishes to thank the International Cooperation Administration, Washington, the International Institute of Nuclear Science and Engineering of the Argonne National Laboratory and U. S. Atomic Energy Commission for providing opportunity to work at the Argonne National Laboratory.